

# EXTREME CLOSE ENCOUNTERS BETWEEN PROTO-MERCURY AND PROTO-VENUS IN TERRESTRIAL PLANET FORMATION

TONG FANG<sup>1</sup> AND HONGPING DENG<sup>2</sup>

<sup>1</sup>*Center of Deep Sea Research, Institute of Oceanology, Chinese Academy of Sciences, Qingdao 266071, China*

<sup>2</sup>*Department of Applied Mathematics and Theoretical Physics, University of Cambridge, Centre for Mathematical Sciences, Wilberforce Road, Cambridge CB3 0WA, UK*

## ABSTRACT

Modern models of terrestrial planet formation require solids to be confined in a narrow annulus at about 0.7-1 astronomical unit (au) initially. Earth and Venus analogs emerge after  $\sim 100$  Myr collisional growth; Mars and Mercury form in the diffusive tails of the annulus. We carried out 250 N-body simulations to study the statistics of close encounters which were recently proposed as an explanation for the high iron mass fraction in Mercury by [Deng \(2019\)](#). We formed 39 Mercury analogs in total and all proto-Mercury analogs were scattered inward by proto-Venus at the late stage of accretion. Proto-Mercury typically experiences 6 extreme close encounters (closest approach smaller than 6 Venus radii) with Proto-Venus after Proto-Venus acquires 0.7 Venus Mass. These encounters are in accordance with the tidal mantle stripping hypothesis ([Deng 2019](#)). However, they seem not frequent and violent enough to fully explain Mercury's high iron fraction. More and closer encounters are expected should tidal dissipation in extreme encounters accounted. Hybrid N-body hydrodynamic simulations, treating orbital and encounter dynamics self-consistently, are desirable to evaluate the probability of tidal mantle stripping of Mercury.

*Keywords:* Terrestrial planets, Mercury, Close encounter

arXiv:2005.05000v1 [astro-ph.EP] 11 May 2020

## 1. INTRODUCTION

The terrestrial planets in our solar system form through collisional growth between planetesimals embedded in a protoplanetary disk (Safronov 1969). The growth of dust to planetesimals under the influence of turbulence in protoplanetary disks remains elusive (see, e.g., review by Testi et al. 2014). The later collisions between planetesimals are readily modeled with N-body simulations (Kokubo & Ida 1998, 2000; Chambers & Wetherill 1998; Morishima et al. 2010). Earth and Venus analogs naturally emerge in N-body simulations (O’Brien et al. 2006) while replicating the smaller planets, Mars and Mercury remains challenging (Raymond et al. 2009). Recent model starting from planetary embryos confined between 0.7-1 au successfully produced Mars and Mercury analogs from the diffusive tails of planetary embryos (Hansen 2009). The initial condition of narrow annulus may be caused by the migration of Jupiter and Saturn in the protoplanetary disk (Walsh et al. 2011) or it can be intrinsic to the planetesimal distribution due to dust drift in protoplanetary disks (Drazkowska et al. 2016; Raymond & Izidoro 2017). The narrow annulus model and its variations are promising with high success rate in replicating Mars and Mercury (Hansen 2009). Alternatively, an eccentric Jupiter (likely caused by giant planet instability, see Clement et al. 2018) can excite the planetesimal disk and form small Mars analogs.

The formation of Mercury, is arguably the most challenging problem in these N-body simulations (Lykawka & Ito 2017; Clement et al. 2019). Mercury also stands out for its anonymously high-iron mass fraction, 70% of the planet mass (Anderson et al. 1987; Hauck et al. 2013) while all other terrestrial planets has only 30% iron by mass. This rocky material deficit may be a result of mantle removal due to giant impacts (Benz et al. 2008; Asphaug & Reufer 2014; Chau et al. 2018) or extreme close encounters with proto-Venus Deng (2019). The high-temperature giant impact scenario seems at odds with the retainment of moderately volatile elements on the present-day Mercury (Peplowski et al. 2011). The multiple encounters scenario avoids high-temperature collisions but whether such extreme close encounters occur repeatedly remains uncertain.

Here we use N-body simulations of terrestrial planet formation to find out whether close encounter between proto-Mercury and proto-Venus occurs. We focus on those extreme encounters which can potentially lead to mantle removal of proto-Mercury. We describe our simulations and present our results in section 2. Discussion follows in section 3. We then conclude in section 4.

## 2. SIMULATIONS AND RESULTS

We used the *Mercury6* package to integrate the planetary embryo system assuming perfect merging upon collisions (Chambers 1999). We chose the confined annulus model of Hansen (2009) because of its high success rate in producing Mercury analogs Clement et al. (2019). This model is chosen also because of its simplicity requiring no extra parameters, for example, parameters for the giant planet migration in the Grand Tack model (Walsh et al. 2011). Initially, the system consists of 400 planetary embryos of equal mass,  $0.005 M_{\oplus}$  (Earth mass) placed between 0.7-1 au representing a uniform distribution of solids Hansen (2009). The density of planetary embryos is assumed to be  $4 \text{ g/cm}^3$ . Jupiter is placed at 5 au with eccentricity = 0.05. We used a timestep of 4 days (Hansen 2009; Lykawka & Ito 2017) and integrated the system for 200 million years (Clement et al. 2019; Kaib & Cowan 2015).

We carried out 250 simulations starting from different realisations of the above solids distribution (Hansen 2009). The evolution of this system is well documented in Hansen (2009) and here we focus on close encounters between Mercury and Venus analogs. At the end of simulations, the large bodies close to 0.7 au and 1 au are identified as Venus and Mercury analogs. We note that we exclude systems left with only one dominant body (typically  $> 1.33M_{\oplus}$ ) and three bodies (typically all larger than  $0.33M_{\oplus}$ ) in later analysis. We formed 39 Mercury analogs ( $a < 0.65 \text{ au}$  and  $M < 0.2M_{\oplus}$ ) and 135 Mars analogs ( $a > 1.3 \text{ au}$  and  $M < 0.2M_{\oplus}$ ) in systems with Venus and Earth analogs clearly identified.

Hansen (2009) has already noted the orbital overlaps between proto-Mercury and proto-Venus in the early stage of planetary accretion (see Figure 6 of Hansen 2009). However, no details about proto-Mercury and proto-Venus encounters are reported therein. All our formed Mercury analogs are scattered inwards by proto-Venus. This is not surprising as the potential well is deep in the inner solar system and thus violent encounters are necessary to shrink proto-Mercury’s orbit. In figure 1, we show the encounter statistics between proto-Mercury and proto-Venus in a typical run. Both Mercury (green curve) and Venus (red curve) analogs accumulate materials quickly and are nearly fully-fledged at 40 Myr. Subsequently, a series of close encounters scatter proto-Mercury inside of proto-Venus. Here we focus on encounters after proto-Venus gains 0.7 Venus mass which can potentially remove proto-Mercury’s mantle (Deng 2019). We term these events as major encounters. In the exemplary run of figure 1, major encounters have a relative velocity at infinity  $v_{\infty} \sim 10 \text{ km/s}$ . In major encounters,  $v_{\infty}$  shows no correlation with the closest ap-

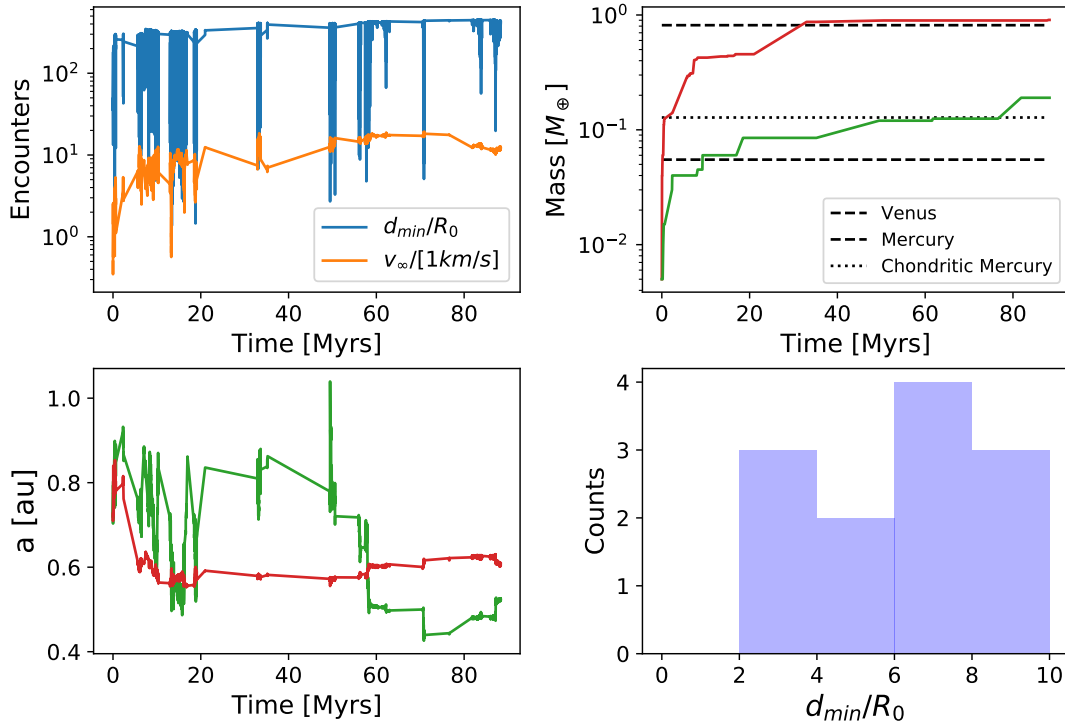


**Figure 1.** Encounters between proto-Mercury and proto-Venus in an exemplary simulation. *Upper left:* the closest approach  $d_{min}$  and the relative velocity at infinity  $v_{\infty}$  for all the close encounter between the formed Mercury and Venus analogs. *Upper right:* mass growth of Mercury and Venus analogs. *Lower left:* semi-major axis of proto-Mercury and proto-Venus at the time of their close encounters. *Lower right:* the number of major encounters with  $d_{min}$  smaller than  $10R_0$  (see text)..

proach,  $d_{min}$  as in other simulations. The value of  $v_{\infty}$  ranges from 2 km/s to 10 km/s for major encounters in our simulations. The frequency of major encounter scales with the square of  $d_{min}$  when  $d_{min}$  is sufficiently large simply reflecting the geometric cross section scaling. We note that all encounters with  $d_{min}$  smaller than three Hill radii are recorded in our simulations. The occurrence rate of major encounter with  $d_{min}$  smaller than  $10R_0$  (Venus radius,  $R_0$ ) is rather irregular so that a statistical study is desirable.

We plot in figure 2 the orbital parameters of all the Mercury analogs. The small Mercury analogs show large scatter in both the semi-major axis and eccentricity. However, there is a clustering of Mercury analogs around 0.5 au and eccentricity = 0.2. This group of Mercury analogs are more massive than Mercury or even a chondritic Mercury (Deng 2019). They also lie too close to Venus analogs (see also Clement et al. 2019, Figure 2). However, they are in line with the tidal mantle stripping model of Deng (2019) as mass transfer to Venus analogs (due to tidal interaction but ignored in N-body simulations) tends to shrink Mercury analog’s semi-major axis towards present-day Mercury value, 0.39 au. The remaining question is whether these encounters are fre-

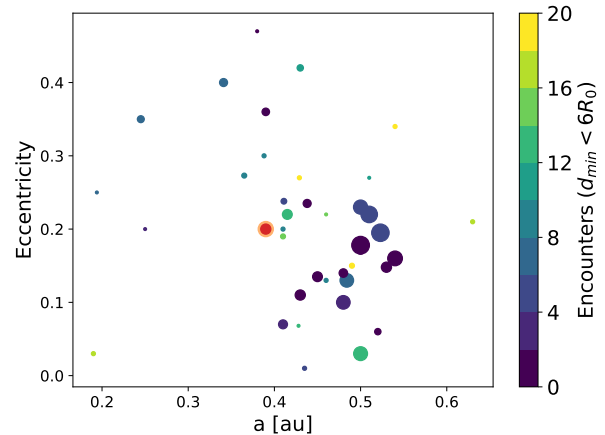


**Figure 2.** Orbital parameters of formed Mercury analogs. The plot consists of 39 Mercury analogs with the Mercury planet indicated by the red circle (the enlarged orange circle indicates a hypothetical chondritic Mercury). The area of the circles scales linearly with the mass of the objects while the color represents their times of major encounters with proto-Venus whose  $d_{min} < 6R_0$  (see Figure 1). We note that Mercury analogs with masses larger than 0.3 Mercury mass have inclinations ( $5^{\circ} - 13^{\circ}$ ) close to present-day Mercury inclination,  $7^{\circ}$ .

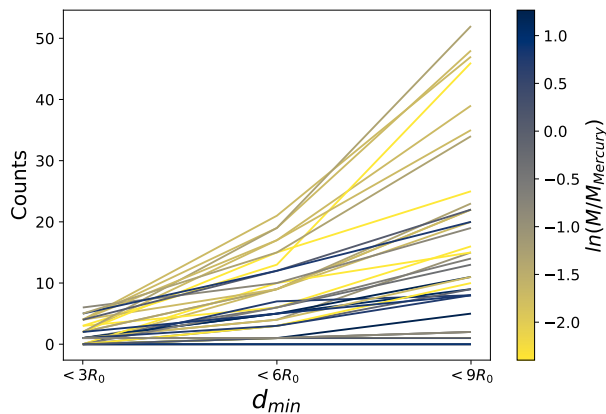


**Figure 3.** The times of proto-Mercury and proto-Venus major encounters (see Figure 1) with  $d_{min} < 3R_0, 6R_0, 9R_0$  respectively. The line colors indicate the mass of the formed Mercury analogs in logarithmic scale. The median of encounter times for  $d_{min} < 3R_0, 6R_0, 9R_0$  are 1, 6, 13 respectively.

quent and violent enough to remove proto-Mercury’s mantle significantly.

We calculated the number of extreme major encounters with  $d_{min}$  smaller than certain values ( $3R_0, 6R_0, 9R_0$ ). It is noteworthy that Venus is able to deflect the orbit of a chondritic Mercury by  $1^\circ$  when  $d_{min} = 9R_0$  and  $v_\infty = 10$  km/s in a test hydrodynamic simulation similar to those of Deng (2019). In figure 3, the lighter Mercury analogs experienced more extreme major encounters in general. There Mercury analogs (0.27, 0.45, 2.18 Mercury mass) have more than 4 times (5, 6, 5) major encounter with  $d_{min} < 3R_0$ . We do not simply take them as successful realisations of the tidal mantle stripping hypothesis of Deng (2019) (see section 3). The median of encounter times for  $d_{min} < 3R_0, 6R_0, 9R_0$  are 1, 6, 13 respectively. Extreme major encounters can dissipate orbital energy and even lead to mass transfer (Deng 2019). Our encounter statistics necessitate proper treatment of tidal interaction in the study of Mercury formation.

### 3. DISCUSSION

We have shown clear evidence of extreme major encounter between proto-Mercury and proto-Venus in N-body simulations of terrestrial planet formation. We refrain from concluding on the probability of proto-Mercury mantle stripping (Deng 2019). During planetary accretion, major encounters happen between Mercury-Venus pairs of different masses,  $v_\infty$ ,  $d_{min}$  and spin. The parameter space explored by Deng (2019) is limited to  $v_\infty < 3$  km/s and  $d_{min} < 2R_0$  so results therein are not

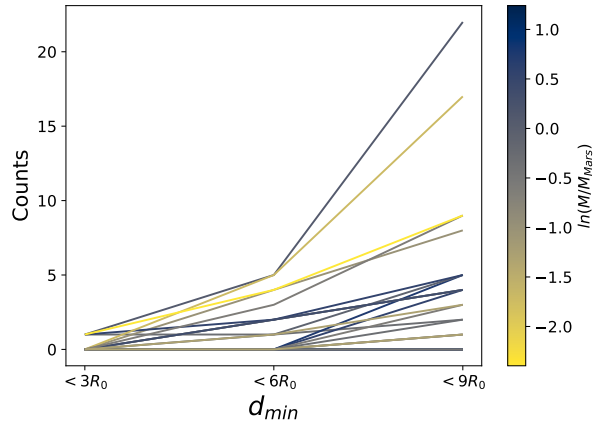


**Figure 4.** The times of proto-Mars and proto-Earth major encounters similar to figure 3. The median of encounter times for  $d_{min} < 3R_0, 6R_0, 9R_0$  are 0, 0, 1 respectively.

fully applicable here. However, we tested that a chondritic Mercury with fast prograde spin can lose part of its mantle to Venus even at  $d_{min} = 3R_0$ . Aside from the limited knowledge in planetary major encounters (due to the high dimensional parameter space) we have not considered all interactions between proto-Mercury and proto-Venus in our analysis above. In figure 1, we only focus on the two objects bearing the identity of the final Mercury and Venus analogs. Embryos merged into the final Mercury analog may have experienced extreme encounter with proto-Venus as well. In this sense, the encounter times discussed above is a lower limit for the study of tidal mantle stripping. Rebuilding the full encounter history between proto-Mercury and proto-Venus is complex and will be addressed in a future paper.

On the other hand, the encounter statistics may not be accurate themselves. As we noted above, tidal dissipation at major encounters tends to bring proto-Mercury closer to proto-Venus (Deng 2019). We expect more encounters at smaller  $d_{min}$  if the dissipation caused by tidal interaction (wave excitation and/or mass transfer) is considered. Hybrid N-body and hydrodynamic simulations are necessary to address the formation of Mercury self-consistently. We may wonder why there is not a metal enriched Mars. Beyond 1 au, the potential well is shallow so less violent encounters can scatter Mars from  $\sim 1$  au to 1.5 au. We carried similar major encounter analysis for 39 randomly chosen Mars analogs (the statistics does not change when more samples are included). In figure 4, we find only about 1 major encounter at  $d_{min} < 9R_0$  between proto-Earth and proto-Mars. Most major encounters have  $d_{min}$  tens of  $R_0$  and  $v_\infty \sim 5$  km/s. In some cases, Mars orbit can even diffuse outwards by indirectly exchanging angular momen-

tum with proto-Earth through smaller objects (Hansen 2009).

The low  $v_\infty$  in close encounters casts further doubt on the single hit-and-run giant impact scenario for Mercury formation which requires a typical impact velocity  $v_{imp} \sim 20$  km/s (Asphaug & Reufer 2014; Chau et al. 2018). Multiple impacts scenario at lower  $v_{imp}$  may reconcile with the observation of moderate volatiles on Mercury more easily than a single impact (Chau et al. 2018). However, repeatedly hit-and-run collisions between proto-Venus and proto-Mercury are much less likely than repeatedly close encounters out of simple geometric cross section consideration.

#### 4. CONCLUSION

We carried out 250 N-body simulations of terrestrial planet formation. We found frequent close encounters between proto-Mercury and proto-Venus after the latter gained 0.7 Venus mass. About 13 such encounters have closest approach smaller than 9 Venus radii. These encounters scatters proto-Mercury to the innermost solar system. However, the formed Mercury analogs have a slightly larger semi-major axis (0.5 au) than present day Mercury value (0.39 au). We expect tidal orbital decay to lead to more violent encounters which eventually remove proto-Mercury’s mantle significantly and bring it further inward.

H.D. acknowledge support from the Swiss National Science Foundation via an early postdoctoral mobility fellowship.

#### REFERENCES

- Anderson, J. D., Colombo, G., Esposito, P. B., Lau, E. L., & Trager, G. B. 1987, *Icarus*, 71, 337
- Asphaug, E., & Reufer, A. 2014, *Nature Geoscience*, 7, 564
- Benz, W., Anic, A., Horner, J., & Whitby, J. A. 2008, in *Mercury* (Springer), 7–20
- Chambers, J., & Wetherill, G. 1998, *Icarus*, 136, 304
- Chambers, J. E. 1999, *Monthly Notices of the Royal Astronomical Society*, 304, 793
- Chau, A., Reinhardt, C., Helled, R., & Stadel, J. 2018, *The Astrophysical Journal*, 865, 35
- Clement, M. S., Kaib, N. A., & Chambers, J. E. 2019, *The Astronomical Journal*, 157, 208
- Clement, M. S., Kaib, N. A., Raymond, S. N., & Walsh, K. J. 2018, *Icarus*, 311, 340
- Deng, H. 2019, *The Astrophysical Journal Letters*, 888, L1
- Drazkowska, J., Alibert, Y., & Moore, B. 2016, *Astronomy & Astrophysics*, 594, A105
- Hansen, B. M. 2009, *The Astrophysical Journal*, 703, 1131
- Hauck, S. A., Margot, J.-L., Solomon, S. C., et al. 2013, *Journal of Geophysical Research: Planets*, 118, 1204
- Kaib, N. A., & Cowan, N. B. 2015, *Icarus*, 252, 161
- Kokubo, E., & Ida, S. 1998, *Icarus*, 131, 171
- . 2000, *Icarus*, 143, 15
- Lykawka, P. S., & Ito, T. 2017, *The Astrophysical Journal*, 838, 106
- Morishima, R., Stadel, J., & Moore, B. 2010, *Icarus*, 207, 517
- O’Brien, D. P., Morbidelli, A., & Levison, H. F. 2006, *Icarus*, 184, 39
- Peplowski, P. N., Evans, L. G., Hauck, S. A., et al. 2011, *science*, 333, 1850
- Raymond, S. N., & Izidoro, A. 2017, *Science advances*, 3, e1701138
- Raymond, S. N., O’Brien, D. P., Morbidelli, A., & Kaib, N. A. 2009, *Icarus*, 203, 644
- Safronov, V. S. 1969, *Evoliutsiia doplanetnogo oblaka*.
- Testi, L., Birnstiel, T., Ricci, L., et al. 2014, *Protostars and Planets VI*, 914, 339
- Walsh, K. J., Morbidelli, A., Raymond, S. N., O’Brien, D. P., & Mandell, A. M. 2011, *Nature*, 475, 206